Tunable, narrow-band, grating-assisted microring reflectors

Carmen Vázquez [a], Otto Schwelb [b,*]

[a] Departamento Tecnología Electrónica, Universidad Carlos III, Leganés 28911, Madrid, Spain
[b] Department of Electrical and Computer Engineering, Concordia University, Montréal, QC, Canada H3G 1M8

ARTICLE INFO

Article history:
Received 26 March 2008
Received in revised form 20 June 2008
Accepted 21 June 2008

Keywords:
Microring resonator
Laser mirror
Optical reflector
Group delay

ABSTRACT

Tunable, grating-assisted ring resonator based optical mirrors are analyzed and their characteristics numerically evaluated. Mode number selection rules are presented to aid mirror optimization for high, narrow-band reflection and efficient sidelobe suppression. Data is presented on tuning sensitivity, on the effect of coupling on bandwidth and reflection coefficient, and on the influence of waveguide and grating loss on mirror performance. Group delay in the presence of loss and circuit parameter variations is also treated.

1. Introduction

Microring resonator based optical mirrors and band-limited reflectors have been the subject of intense investigations in recent years, primarily as a result of advancements in fabrication technology and miniaturization of integrated devices [1–6]. In this paper we present analytical and simulated results on the performance of three closely related narrow-band laser mirror configurations which use Bragg gratings to confine their operating range. The gratings provide the means to suppress repetition of the reflection spectrum at every free spectral range (FSR) removed from the design wavelength, and permit a laser with a wide gain characteristic to oscillate at several frequencies. The device consists of a single microring resonator and two identical Bragg gratings as shown in Fig. 1. It can be viewed as a phase shifted Fabry–Pérot resonator that uses gratings as mirrors and a coupling mechanism to transfer its spectrum to the laser that includes a microring. The difference between the configurations shown in Fig. 1 is in the method the gratings are attached to the microring. One of the configurations has been discussed in a different context in [7–10] while another was briefly treated in [11]. Although the three variants appear to be similar, their characteristics and fabrication differ in respects that determine the choice of application. For example, the type I mirror of Fig. 1 indicates geometry where the connection between the resonator and the Bragg gratings might require very small bending radii and consequently precision waveguide fabrication to avoid excessive radiation loss. Resolution of this problem is offered in the type III mirror configuration which, however, requires vertically displaced waveguides and the associated more critical fabrication technology. Tunability, bandwidth (BW), sidelobe suppression (SS), sensitivity to loss and the most convenient placement of (thermo-optic) tuning pads are other aspects differentiating the three configurations.

In Section 2 we present a network analysis of the reflectors and plot the spectral characteristics of the reflected intensity. Here we also discuss the selection rules that determine the optimum mode numbers of the ring and the grating arms. Tuning sensitivity is treated in Section 3 while in Section 4 BW and the effects of waveguide and grating loss on reflectivity are presented. Section 5 is devoted to computed results on group delay in reflection [12] and in Section 6 we draw some conclusions.

2. Analysis and spectral characteristics

The common circuitry of the reflector configurations are depicted schematically at the top part of Fig. 1, showing the bus waveguide with input and output ports, the microring with circumference L, the gratings, and the two couplers K_c and K. At the bottom of this figure are shown, for the three reflector configurations, the direct (solid lines) and coupled (dotted lines) connections within the coupler denoted by K. Accordingly, in the type I mirror the ring section $(1-h)L$ is directly connected to arm l_3 and hL to l_4, whereas in the type III mirror the reverse is true. In the type II mirror one of the direct connections closes the ring while the other connects the two gratings, thus when the coupling is reduced to zero the gratings are completely separated from the ring.

* Corresponding author. Tel.: +1 514 573 9155; fax: +1 514 848 2802.
E mail addresses: cvazquez@ing.uc3m.es (C. Vázquez), otto@ece.concordia.ca (O. Schwelb).

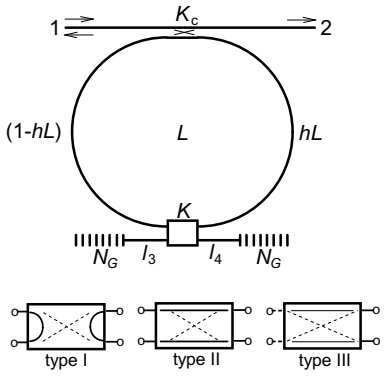

Fig. 1. Three types of grating-assisted microring resonator mirrors. The direct and coupled connections of the coupler *K*, detailed at the bottom, are indicated by the solid and dotted lines, respectively. The ring perimeter is *L*, N_G is the number of periods in each grating, and h $(0 < h < 1)$ locates the coupler *K* on the ring. The attenuation coefficient of the waveguides is α, the ring need not be circular.

K represents the power coupling coefficient of the bottom coupler, and K_c that of the coupler between the ring and the bus waveguide. The location of *K* within the ring, determined by h $(0 < h < 1)$, is arbitrary. We assume that all four waveguide sections, namely hL, $(1 \quad h)L$, l_3 and l_4, are characterized by the same effective refractive index n_{eff} and the same amplitude attenuation coefficient α, although these restrictions can easily be relaxed. We also admit localized or distributed gain in the ring [13 15] and thermo optic length or refractive index adjustment [16,17] for L, l_3, l_4 and n_{eff}. All optical lengths are given in terms of mode numbers, thus N $Ln_{\text{eff}}/\lambda_0$ and $n_i \quad l_i n_{\text{eff}}/\lambda_0$, $i \quad 3, 4$, where $\lambda_0 \quad c/f_0$ is the design wavelength and c the velocity of light in vacuum. The gratings are identical, quarter wavelength shallow gratings, meaning that the relative index difference $(n_b \quad n_a)/n_a << 1$, $(n_b > n_a)$. The gratings are characterized by the grating strength $GS \quad N_G(n_b \quad n_a)/n_a$ where N_G is the number of periods. Balanced operation is ensured by selecting $K \cong 0.5$, while K_c must be small to prevent loading and to preserve the resonance spectrum of the grating assisted ring [18]. Here we remark that the type II mirror of Ref. [11], using $K_c \quad 0.5$ and $0.01 \leqslant K \leqslant 0.05$ also produces a very high SS, relatively low reflection loss (RL) mirror. Coupling scheme differences result in significant diversity in performance as well as demands on fabrication. Foremost among these is the extremely large SS and the heightened sensitivity to *K* in the vicinity of $K \quad 0.5$, observed in type I mirrors for a particular mode number combination, as described below.

To simplify the analysis we combine the coupler *K* and the two gratings, including their arms l_3 and l_4, into a single two port network characterized by its scattering matrix $\boldsymbol{S}_K$ which can be calculated from first principles and is found to be

$$\boldsymbol{S}_K \quad \begin{bmatrix} c^2\Gamma_3 & s^2\Gamma_4 & \mathrm{j}sc(\Gamma_3+\Gamma_4) \\ \mathrm{j}sc(\Gamma_3+\Gamma_4) & c^2\Gamma_4 & s^2\Gamma_3 \end{bmatrix} \tag{1}$$

for the type I configuration,

$$\boldsymbol{S}_K \quad \frac{1}{1 \quad c^2\Gamma_3\Gamma_4}\begin{bmatrix} s^2\Gamma_4 & c(1 \quad \Gamma_3\Gamma_4) \\ c(1 \quad \Gamma_3\Gamma_4) & s^2\Gamma_3 \end{bmatrix} \tag{2}$$

for the type II configuration, and

$$\boldsymbol{S}_K \quad \frac{1}{1+s^2\Gamma_3\Gamma_4}\begin{bmatrix} c^2\Gamma_4 & \mathrm{j}s(1+\Gamma_3\Gamma_4) \\ \mathrm{j}s(1+\Gamma_3\Gamma_4) & c^2\Gamma_3 \end{bmatrix} \tag{3}$$

for the type III configuration, where $c \quad (1K)^{1/2}$, $s \quad (K)^{1/2}$, and

$$\Gamma_i \quad \frac{\mathrm{j}\kappa^* \mathrm{sh}(\gamma_G N_{G,i}\Lambda)}{\gamma_G \mathrm{ch}(\gamma_G N_{G,i}\Lambda) + (\alpha+\mathrm{j}\Delta\beta)\mathrm{sh}(\gamma_G N_{g,i}\Lambda)} \exp[\ 2(\alpha+\mathrm{j}\beta)l_i] \tag{4}$$

$i \quad 3, 4$ are the complex reflection coefficients of arms 3 and 4, consisting of guide lengths l_3 and l_4, respectively, terminated by their corresponding gratings of lengths $N_{G,i}\Lambda$, where Λ is the periodicity, $\Delta\beta \quad \beta \quad \pi/\Lambda$ is the detuning, α is the amplitude attenuation in the waveguides, $\gamma_G \quad [|\kappa|^2 + (\alpha + \mathrm{j}\Delta\beta)^2]^{1/2}$ and κ is the coefficient that measures the coupling between forward and backward traveling waves in the grating [19].

The relevant elements of the scattering matrix $\boldsymbol{S}$ of the entire reflector are the reflection coefficient S_{11} and the transmission coefficient S_{21}, both complex valued functions of frequency. Assuming $\alpha \quad 0$ and $h \quad 0.5$, tedious but straightforward algebra yields

$$S_{11} \quad \frac{s_c^2 S_{K,22}[c_c S_{K,21}\mathrm{e}^{\mathrm{j}\beta L/2} \quad c_c S_{K,21} \quad \mathrm{e}^{\mathrm{j}\beta L}]}{1 \quad 2c_c S_{K,21} \quad c_c^2 \det(\mathbf{S}_K)} \tag{5}$$

and

$$S_{21} \quad c_c + \frac{s_c^2\left[c_c S_{K,21}^2 \mathrm{e}^{\mathrm{j}\beta L/2} \quad c_c S_{K,11}S_{K,22} \quad S_{K,21}\mathrm{e}^{\mathrm{j}\beta L}\right]}{1 \quad 2c_c S_{K,21} \quad c_c^2 \det(\boldsymbol{S}_K)} \tag{6}$$

where $c_c \quad (1K_c)^{1/2}$, $s_c \quad (K_c)^{1/2}$ and $\det(\mathbf{S}_K) \quad \Gamma_3\Gamma_4$, $(\Gamma_3\Gamma_4 \quad c^2)/(1 \quad c^2\Gamma_3\Gamma_4)$ or $(\Gamma_3\Gamma_4 + s^2)/(1 + s^2\Gamma_3\Gamma_4)$, for mirror types I, II or III, respectively. When dealing with lossy waveguides β must be replaced by $\beta \quad \mathrm{j}\alpha$. When a semiconductor optical amplifier (SOA) is embedded in the ring to compensate losses, a negative α can be used such that its product with the perimeter length *L* equals the gain of the SOA.

Denoting the reflected and transmitted intensity of the reflectors by $I_{11} \quad |S_{11}|^2$ and $I_{21} \quad |S_{21}|^2$, respectively, the computed spectral response of the lossless devices are plotted in Figs. 2 4 for three values of the resonator mode number *N*, as a function of detuning from the design frequency f_0, the center frequency of the grating passband. In our calculations we used $K_c \quad 0.02$, $K \quad 0.4944$, $N_G \quad 600$ $(GS \quad 3.92)$, a center wavelength of $\lambda_0 \quad 1.579$ μm and $n_{\text{eff}} \quad 4.5$, appropriate for SOI waveguides [20].

There are two kinds of type I mirrors, namely the very large SS variety whose spectrum is shown in Fig. 2 and the moderate SS variety whose spectrum appears in Fig. 3. They differ in the mode number of one of the grating arms, i.e., in the relative reflection phase of the grating reflectors. The difference is 180°, so for

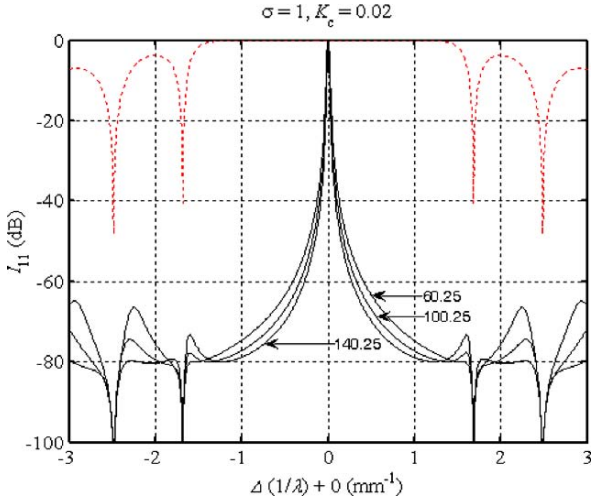

Fig. 2. Reflected intensity of the type I mirror for three mode numbers when $n_3 = n_4 = 10.25$. Also shown (dotted line) is the reflection loss characteristics of the gratings. $N_G = 600$, $n_a = 4.5294$, $n_b = n_{\text{eff}} = 4.5$ $(GS = 3.92)$, $K = 0.4944$, $K_c = 0.02$, $\lambda_0 = 1.5791$ μm and $\sigma = \exp(\alpha L)$. Multiply the abscissa by 3×10^2 to obtain the detuning in GHz. As $|K - 0.5| \to 0$ the SS increases.

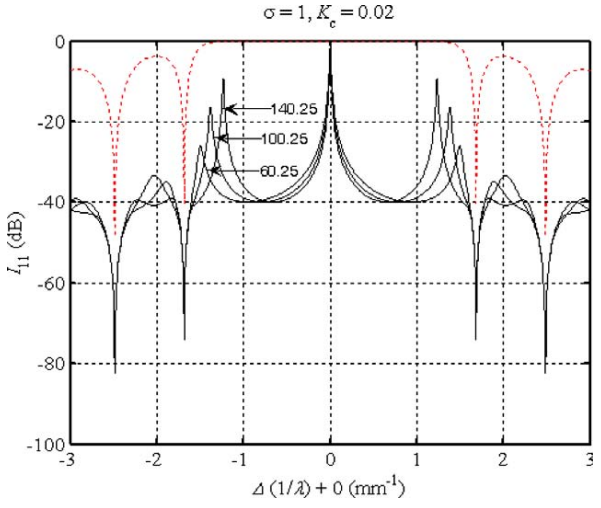

Fig. 3. Reflected intensity of the type I mirror for three mode numbers when $n_3 = 10.25$ and $n_4 = 10$. All other parameters are the same as in Fig. 2. Notice the reduced SS, virtually independent of K, in comparison to Fig. 2.

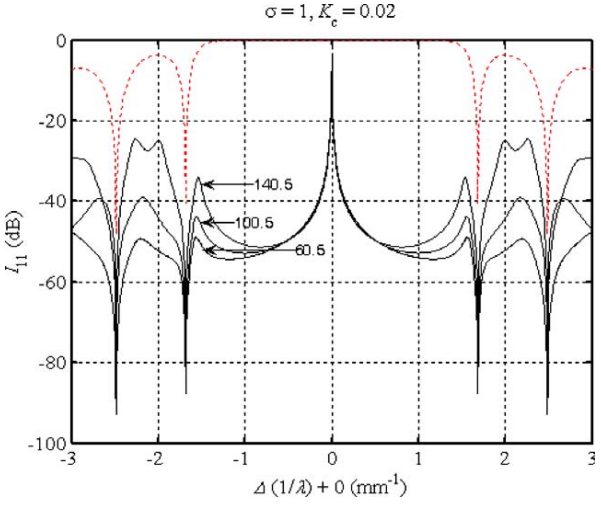

Fig. 4. Reflected intensity as a function of detuning for the type II mirror. The parameter is the mode number of the ring, n_3 (n_4) = 10 or 10.5, while the other parameters are the same as in Fig. 2. In the vicinity of $K = 0.5$ the response is virtually independent of K. This characteristic also applies to type III mirrors, but with a different set of mode numbers (see Table 1).

example in Fig. 2 n_3 n_4 10.25, whereas in Fig. 3 n_3 10.25 and n_4 10, or vice versa. In addition to the significantly larger SS this π phase shift also results in a strong dependence of the SS on K as $|K$ 0.5| approaches zero in Fig. 2, whereas the response in Fig. 3 is virtually insensitive to K. Furthermore, as we demonstrate below, the settings of Fig. 2 allow for the shaping of the resonance peak by adjusting K. The characteristics of the type II mirror are shown in Fig. 4, indicating significantly larger SS than that displayed in Fig. 3 but similar insensitivity to K. The plots of Fig. 4 also apply to type III mirrors using appropriate mode numbers. In all three configurations the location of the bottom coupler, the value of h in Fig. 1, affects only the phase of S_{11}.

Figs. 3 and 4 indicate an improvement of the SS with decreasing mode number N. This is due to the inverse relationship between mode number and free spectral range (FSR f_0/N) and the atten dant shift of the adjacent resonances into regions with increased grating rejection. If reducing the mode number N to obtain higher SS is for some reason undesirable, apodized gratings yielding de pressed sidelobes can be used instead of uniform ones.

Observe that the mode numbers are not integers. They must be selected to provide adequate sideband suppression and a (nearly) centered reflection spectrum. The selection rules are determined by the phase shifts within the couplers and the grating arms, and by the imperative for constructive interference at the input port at f_0. Consider that in a type I mirror the gratings are connected through the ring both clockwise and counter clockwise incurring a phase shift difference of 180°. In a type II mirror the gratings are connected both directly and also through the ring, in which case an extra 180° phase shift is incurred by crossing the coupler twice. Finally, in a type III mirror the gratings are connected through the ring and through the coupler incurring a 90° phase dif ference between them. The reflection phases of the gratings, which are subject to their construction, determine the selection rules for n_3 and n_4. In our simulations we used the *HLHLH* sequence, where H, the high refractive index was 1.0065 times the low refractive in dex L. These characteristics explain the nature of the mode number selection rules listed in Table 1, where I represent an arbitrary po sitive integer.

The type I mirror, as represented by the spectrum of Fig. 2, dif fers from the others in the effect small variations of K (≈0.5) have on the resonant response in the vicinity of f_0. This is illustrated in Fig. 5, where details of the resonance peaks of Figs. 2 and 3, for four values of K are compared assuming lossless waveguides and a com mon K_c. The results show that (a) the high SS type I mirror has stee per rolloff than its moderate SS alternative, and (b) that it displays the typical overcoupling/undercoupling effects of a discontinuity assisted ring [21] near critical coupling: $K_{c,crit}$ $2r/(1 + r)$, where r $|S_{K,22}|$ is the (2,2) element of (Eq. (1)). In the present example, using K 0.4944, $r(f_0)$ 0.0112 and $K_{c,crit}$ 0.02215 which is

Table 1
Mode number selection rules; I is an arbitrary positive integer

Description	N	n_3	n_4
Type I mirror, very large SS, very sensitive to K	$I + 1/4$	$n_3 = I \pm 1/4$	$n_3 = I \pm 1/4$
	$I - 1/4$	$n_3 = 1/2I$	$n_4 = 1/2I$
Type I mirror, moderate SS, insensitive to K	$I \pm 1/4$	$n_3 + n_4 = I \pm 1/4$	
Type II mirror, high SS, insensitive to K	$I \pm 1/2$	$n_3 + n_4 = 1/2I$	
Type III mirror, high SS, insensitive to K	$I - 1/4$	$n_{3,4} = 1/2I$	$n_{4\,3} = I \pm 1/4$

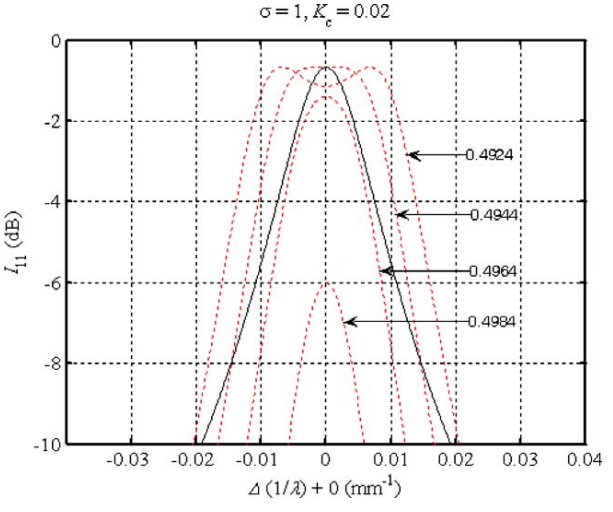

Fig. 5. Passband center of the lossless type I mirror for four values of K. Dotted lines: $n_3 = n_4 = 10.25$, solid line: $n_3 = 10.25$, $n_4 = 10$ (adjustment in K has no effect on the response). $K_c = 0.02$, $N = 60.25$, $GS = 3.92$.

exactly the value where critical coupling is observed. The effect of varying K_c, applied to reflectors using ring resonator mode numbers 60.25 and 140.25 is displayed in Fig. 6, showing the resonance broadening effect of ring diameter reduction, as well as the fact that a change in N does not affect the RL. To illustrate the sensitivity of the resonance characteristics the range of K values that provide a reasonably flat (with a maximum of 3 dB ripple) resonance peak for the lossless, high SS, type I mirror are summarized in Table 2 for four values of K_c.

To compare the RL, the BW and the mode number dependence of the BW, between high SS type I and type II mirrors, we plotted in Fig. 7, using the same K_c and N values as in Fig. 6, the reflected intensity of the type II mirror. Notice that decreasing N from 140 to 60 hardly affects the BW, and that in the type II mirror there is no overcoupling/undercoupling phenomenon. In fact this phenomenon exists only in the high SS type I mirror on account of the competition between reflected waves re entering the ring from the bottom coupler. A diagram of the reflected intensity in type III mirrors, using N 140.75 and N 60.75 with n_3 10, n_4 10.25, α 0 and GS 3.92 exhibits results that are very similar to those of Fig. 7. We shall discuss the sensitivity of f_0 to incremental changes in mode numbers in the next Section on tunability.

3. Tuning sensitivity

When one of the three mode numbers: N, n_3 or n_4 is incrementally altered the resonance frequency is expected to shift. As we shall see below that this is not always the case. Calculations show that shifts of the central resonance are at least two orders of magnitude less sensitive to changes in the coupling coefficients than to changes in mode numbers, and that waveguide attenuation has no effect on f_0. For the high SS type I mirror the evolution of the reflected intensity response as N decreases from 50.25 to 50.0 in increments of 0.05, covering a frequency span of approximately 300 GHz, appears in Fig. 8. This translates to $\delta f \approx 1.2$ GHz downshift for δN 1×10^{-3}, very close to the computed value of 1.26 GHz. In high SS mirrors the effect of an incremental change in N results simply in a shift of f_0, while a change in n (n_3 or n_4) also creates some overcoupling, i.e., affects the shape of the peak.

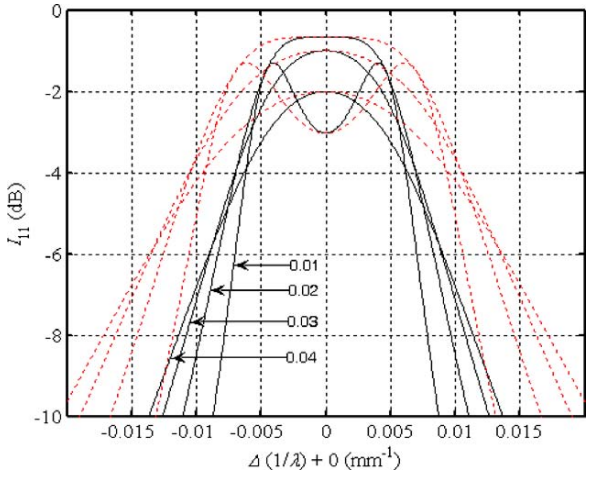

Fig. 6. Resonance peaks of lossless type I mirror. Solid lines: $N = 140.25$, dotted lines: $N = 60.25$, $n_3 = n_4 = 10.25$, $GS = 3.92$, K_c is the parameter (solid and dotted plots with the same extrema correspond to the same K_c).

Table 2
Useful range of K for lossless, high SS, type I mirror

K_c	Upper limit of K	Lower limit of K
0.01	$0.5 \pm 2 \times 10^{-3}$	$0.5 \pm 6 \times 10^{-3}$
0.02	$0.5 \pm 3 \times 10^{-3}$	$0.5 \pm 12 \times 10^{-3}$
0.03	$0.5 \pm 4 \times 10^{-3}$	$0.5 \pm 18 \times 10^{-3}$
0.04	$0.5 \pm 5 \times 10^{-3}$	$0.5 \pm 24 \times 10^{-3}$

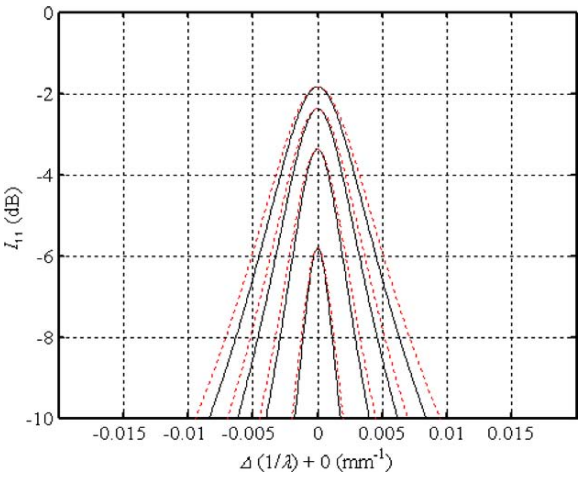

Fig. 7. Resonance peaks of lossless type II mirror. Solid lines: $N = 140.5$, dotted lines: $N = 60.5$, n_3, $n_4 = 10$ or 10.5, $GS = 3.92$, $K_c = 0.01$, 0.02, 0.03, 0.04, the larger the K_c the smaller the RL and the wider the band. Very similar characteristics apply to type III mirrors with corresponding mode numbers.

Morphing of low into high SS state in a lossless type I mirror is demonstrated in Fig. 9, showing the effect of the increase of n_3 from 10 to 10.25 in increments of 0.05, while N 50.25, n_4 10.25, K_c 0.02 and N_G 600 (GS 3.92). Here we observe that incrementation of n_3 does not shift f_0.

Like their spectral characteristics, type II and type III mirrors also share similar tuning sensitivities. We found the grating arms nearly six times as sensitive to fractional changes in the optical length ($n_{eff}l$) than the microring. In particular, for N 50.5 (n_3 0, n_4 0) we obtained a downshift of δf 2.22 GHz for δn 1×10^{-3} or δN 5.9×10^{-3} (type II mirror), and for N 50.75 (n_3 0.25,

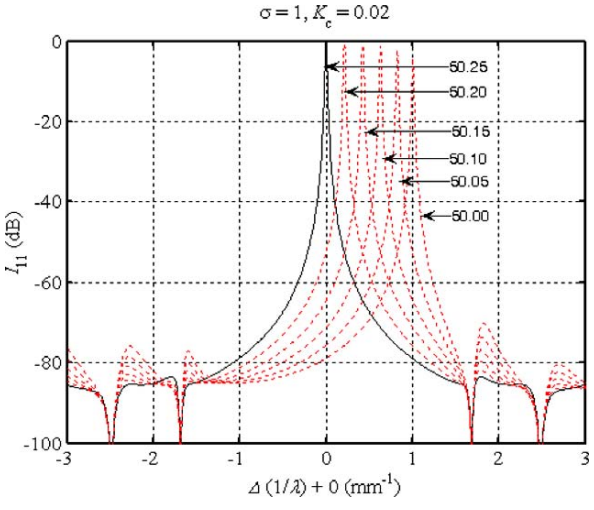

Fig. 8. The evolution of the reflected intensity spectrum in type I mirror. The parameter is N, $n_3 = n_4 = 10.25$, $K = 0.4944$, $\alpha = 0$, $N_G = 600$, $GS = 3.92$. When $N = 50$, $\delta f \approx 1.28$ GHz for $\delta N = 1 \times 10^{-3}$.

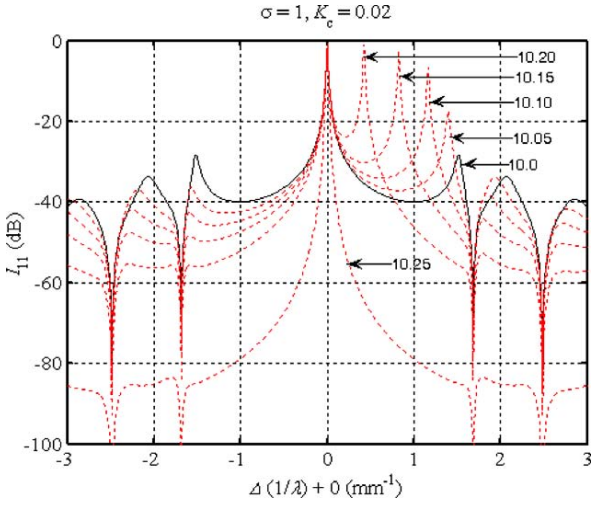

Fig. 9. Type I mirror. Morphing of low into high SS as n_3 increases from 10 to 10.25. $N = 50.25$, $n_4 = 10.25$, $K = 0.4944$, $\alpha = 0$, $N_G = 600$, $GS = 3.92$. Notice that the resonant peak at f_0 remains fixed.

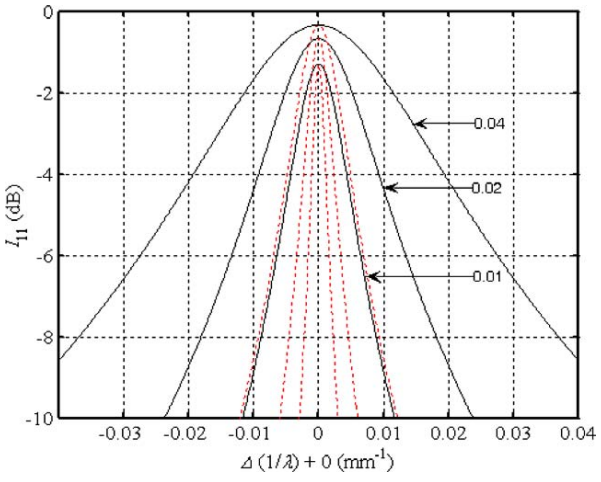

Fig. 10. The effect of K_c on BW. Solid lines: moderate SS type I mirror, $N = 50.25$, $n_3 = 0$, $n_4 = 0.25$, $N_G = 600$, $\alpha = 0$, dash-dot lines: type II mirror, $N = 50.5$, $n_3 = 0$, $n_4 = 0$, $N_G = 736$, $\alpha = 0$, (curves having the same maxima belong to the same K_c). Characteristics for the type III mirror are virtually identical to those of the type II mirror.

n_4 0) a downshift of δf 2.21 GHz resulted for δn 1×10^{-3} or δN 5.74×10^{-3} (type III mirror).

4. Bandwidth and reflection loss

The BW of the resonant peak at f_0 is affected by the combined value of the mode numbers $(N + n_3 + n_4)$ and by the external coupling coefficient K_c. Waveguide attenuation, and/or grating loss through leakage, depresses the peak but does not directly affect the BW. Small changes in K have noticeable effect on the BW only in the high SS type I mirror, through overcoupling or undercoupling, as displayed in Fig. 5.

In general terms, increasing the combined mode number and/or decreasing K_c reduces the BW. Since [22]

$$Q \quad \frac{f_0}{BW} \quad \frac{2\pi N}{K_c + 2T_G + 2\alpha L} \overset{\alpha \ 0}{\rightarrow} \frac{2\pi N}{K_c + 2T_G} \tag{7}$$

where T_G denotes the power loss through a grating, these results meet expectations. A decrease in the value of K_c also reduces the peak value of the resonance, because with reduced coupling less external power is needed to maintain cavity oscillation. Some of these effects are displayed below. Fig. 10 shows that the BW of type II (as well as type III) mirrors are significantly less sensitive to K_c than that of the type I configuration. Note that the reflection coefficients of the gratings of the type II (type III) mirrors have been adjusted to provide the same band center loss as the type I mirror. Fig. 11 plots the resonance peak in type I and type II (type III) mirrors for three nominal mode numbers using K_c 0.02. Here we observe that the BW spread in the latter configurations is once again significantly smaller than that in the former.

Reflection loss, defined as the level of the reflected intensity relative to the incident intensity, i.e., $|S_{11}|^2$, depends on the leakage through the gratings determined by the GS, the resonator loss and the power escaping through port 2, i.e., $|S_{21}|^2$. Power conservation requires that the sum of these four components equals the input power entering port 1. Resonator loss is determined by the per turn power loss $2\alpha L$, but reaches a peak at f_0 due to resonant enhancement. Transmission loss also peaks at f_0 [22]. If there is no leakage through the gratings due to a very large GS, the RL is a function of α, L and K_c. In contrast, when waveguide loss is negligible and the RL is driven by leakage through the gratings,

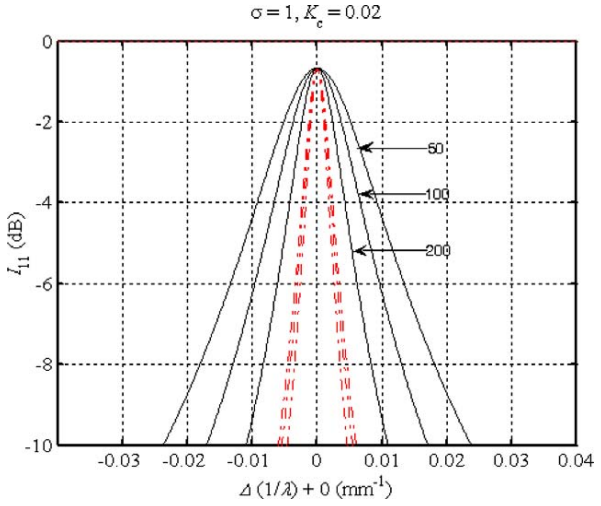

Fig. 11. The effect of N on BW. Solid lines: moderate SS type I mirror, $n_3 = 0$, $n_4 = 0.25$, $N_G = 600$, dash-dot lines: type II mirror, $n_3 = 0$, $n_4 = 0$, $N_G = 736$, $K_c = 0.02$, $\alpha = 0$. The parameter is the nominal mode number, the smaller the N the wider is the BW. Type II and type III mirror responses are virtually identical.

only K_c and the GS affect RL. In any event, loss within the ring and leakage through the gratings reach a maximum while output at port 2 dips to a minimum at resonance. Fig. 12 plots for type I and for type II mirrors the RL as a function of α for three values of K_c when there is no leakage through the gratings (N_G 2000, GS 13), K 0.5 and the nominal mode numbers are N 100, and n_3 n_4 0, respectively. Similarly, Fig. 13 is a RL $RL(GS)$ plot for type I and type II mirrors of the same description when α 0. The responses of type III mirrors are not shown because they are very similar to those of the corresponding type II mirrors. The diagrams show that type I mirrors have significantly smaller RL than the other types, and that increasing K_c reduces RL. (Note that we use a positive number for loss, a negative level.)

Referring to Figs. 12 and 13 we note that identical αL products do not ensure identical RL at f_0, however the RL is independent of N when it is driven by leakage loss (α 0). Also, the output level at port 2, i.e., $|S_{21}|^2$ at resonance rises with rising resonator loss

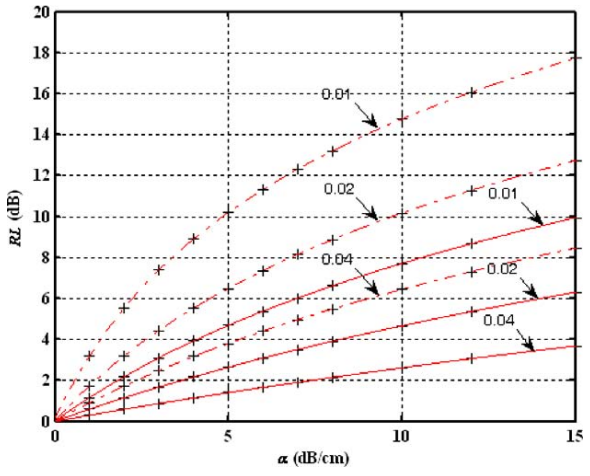

Fig. 12. Computed reflection loss at f_0 in type I (solid lines) and type II (dash-dot lines) mirrors as a function of α. The nominal mode numbers are: $N = 100$, $n_3 = n_4 = 0$, $GS = 13$, $K = 0.5$. The parameter is K_c. The properties of the type III mirror are the same as those of the type II mirror.

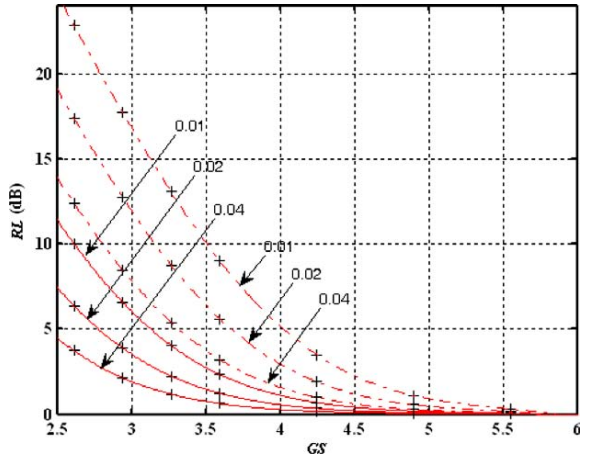

Fig. 13. Computed reflection loss at f_0 in type I (solid lines) and type II (dash-dot lines) mirrors as a function of the GS. The nominal mode numbers are: $N = 100$, $n_3 = n_4 = 0$, $\alpha = 0$, $K = 0.5$, the parameter is K_c. The characteristics of the type III mirror are the same as those of the type II mirror.

and/or rising leakage through the gratings, a phenomenon which at first glance seems counterintuitive and indicates a partition between the reflected power on the one hand and the absorbed and transmitted power on the other. Finally, we note that for the same level of internal or leakage loss, the transmitted power levels at port 2 are always (significantly) higher in type II and type III mirrors than for the type I mirror.

5. Group delay in reflection

We also computed the group delay in reflection: τ_{11}, for lossless and moderately lossy reflectors, for several coupling coefficients K_c. The group delay was computed from (Eq. (5)) using the expression [22]

$$\tau_{11} \quad \mathrm{Im}\left[\frac{1}{S_{11}}\frac{\partial S_{11}}{\partial \omega}\right] \tag{8}$$

The group delay in reflection is plotted in Fig. 14, over the central region of the passband, for high and moderate SS type I mirrors for several values of K. The dotted curves show the effect of slight

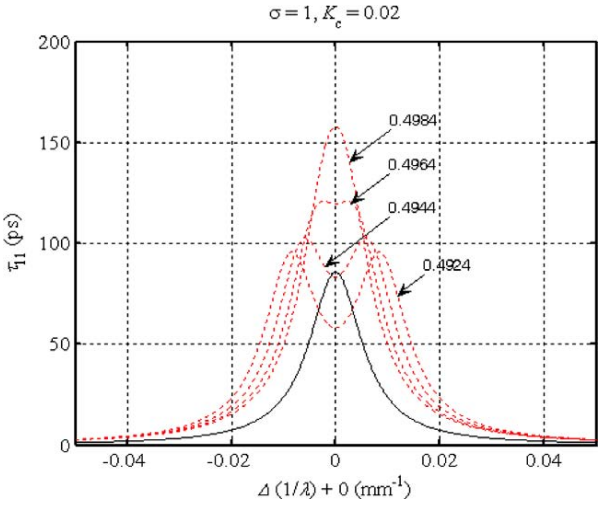

Fig. 14. Group delay in reflection of type I mirrors, $\alpha = 0$, $N = 100.25$, $N_G = 600$ ($GS = 3.92$), $K_c = 0.02$, the parameter is K. Dotted lines: $n_3 = n_4 = 0.25$ (high SS), solid line: $n_3 = 0.25$, $n_4 = 0$ (same plot for all four K values).

changes in K in the high SS configuration, while the single solid line shows that adjustment of K, while $K \approx 0.5$, has no effect on τ_{11} in the moderate SS case. Notice that the coefficient K 0.4944, found to provide critical coupling for I_{11} at K_c 0.02 in the high SS type I mirror, does not provide flat top τ_{11} characteristic. Instead, flat top τ_{11} characteristic is obtained for K 0.4964. Fig. 15 plots τ_{11} for high SS (dotted lines) and moderate SS (solid lines) type I mirrors, using K 0.4944, for three microring mode numbers. Both Figs. 14 and 15 were computed using α 0, K_c 0.02, N_G 600 (GS 3.92) and vanishing grating arm lengths. Group delay in reflection in type II and type III mirrors show the same single peak characteristic as those of the solid lines in Figs. 14 and 15. Peak values of τ_{11} in ps, obtained assuming α 0 and 4 dB/cm, N_G 600 (GS 3.92) and K 0.5 are listed in Table 3 for moderate SS type I and for type II mirrors indicating significantly larger group delays for the latter. Corresponding values for type III mirrors (n_3 0, n_4 0.25) were found to be very close to those of type II mirrors. Since, if used as a laser mirror, τ_{11} contributes to its photon lifetime, a larger

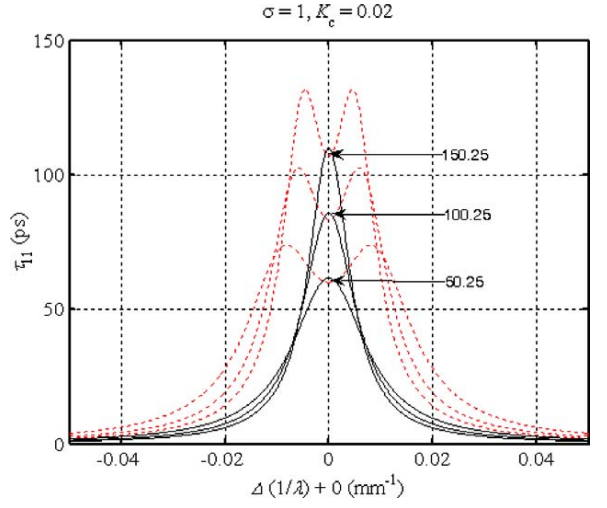

Fig. 15. Group delay in reflection of lossless type I mirrors. Solid curves: moderate SS ($n_3 = 0.25$, $n_4 = 0$), dotted curves: high SS ($n_3 = n_4 = 0.25$). The parameter is N, $N_G = 600$ ($GS = 3.92$), $K_c = 0.02$, $K = 0.4944$.

Table 3
Peak group delay in reflection in ps

Nominal N	α (dB/cm)	$K_c = 0.01$	$K_c = 0.02$	$K_c = 0.04$
50	0	115.3	61.7	31.7
		269.8	177.5	104.6
	4	85.2	51.9	28.9
		147.8	115.0	79.3
100	0	160.4	85.8	44.1
		296.8	195.2	115.1
	4	107.6	68.0	38.9
		155.6	122.2	85.1

$N_G = 600$, $GS = 3.92$, $K = 0.5$. Top figures: moderate SS type I mirror ($n_3 = 0$, $n_4 = 0.25$), bottom figures: type II mirror ($n_3 = n_4 = 0$). Delays in type II and III mirrors are the same.

group delay in reflection raises the Q and narrows the line width. As can be gleaned from Table 3, whether it is caused by waveguide attenuation or by leakage through the gratings, loss flattens the τ_{11} characteristics and reduces its peak.

6. Conclusions

Three grating assisted ring resonator based narrow band optical reflectors have been analytically and numerically examined. The grating pair is instrumental in enabling a single microring to be used as a mirror free of a repetitive spectrum. Reflection and group delay characteristics have been presented and the effects of waveguide loss and leakage through finite length gratings evaluated. Tuning sensitivity in response of optical length ($n_{\text{eff}}L$) variations in both the microring and the grating arms was investigated. We also examined shaping the peak of the resonance characteristic of the high SS type I mirror and found it feasible at a cost of the technologically challenging fine adjustment of K. Among the mirror configurations examined significant differences have been found in SS, in BW, in RL, in group delay, and in the sensitivity to deviations in K. These differences and the potential radiation loss associated with small bending radii used in one design are expected to guide the designer.

Acknowledgments

The support of the Spanish Ministry of Education project CICYT TEC2006 13273 C03 03/MIC and of the Natural Sciences and Engineering Research Council of Canada are acknowledged.

References

[1] B. Liu, A. Shakouri, J.E. Bowers, IEEE Photon. Technol. Lett. 14 (2002) 600.
[2] J.K.S. Poon, J. Scheuer, A. Yariv, IEEE Photon. Technol. Lett. 16 (2004) 1331.
[3] I. Chremmos, N. Uzunoglu, IEEE Photon. Technol. Lett. 17 (2005) 2110.
[4] Y. Chung, D.-G. Kim, N. Dagli, IEEE Photon. Technol. Lett. 17 (2005) 1773.
[5] .G.T. Paloczi, J. Scheuer, A. Yariv, IEEE Photon. Technol. Lett. 17 (2005) 390.
[6] O. Schwelb, J. Lightwave Technol. 23 (2005) 3931.
[7] C. Vázquez, S. Vargas, J.M.S. Peña, Appl. Opt. 39 (2000) 1934.
[8] C. Vázquez, S. Vargas, J.M.S. Pena, P. Corredera, IEEE Photon. Technol. Lett. 15 (2003) 1085.
[9] C. Vázquez, J. Montalvo, P.C. Lallana, J.M.S. Pena, Proc. SPIE 5840 (2005) 315.
[10] C. Vázquez, S. Vargas, J.M.S. Pena, J. Lightwave Technol. 23 (2005) 2555.
[11] O. Schwelb, IEEE Trans. Microwave Theory Tech. 46 (1998) 1409.
[12] G. Lenz, B.J. Eggleton, C.K. Madsen, R.E. Slusher, IEEE J. Quantum Electron. 37 (2001) 525.
[13] B. Vizoso, C. Vázquez, R. Civera, M. López-Amo, M.A. Muriel, J. Lightwave Technol. 12 (1994) 294.
[14] D.G. Rabus, M. Hamacher, U. Troppenz, H. Heidrich, IEEE Photon. Technol. Lett. 14 (2002) 1442.
[15] O. Schwelb, I. Frigyes, Microwave Opt. Technol. Lett. 42 (2004) 427.
[16] M.W. Pruessner, T.H. Stievater, M.S. Ferraro, W.S. Rabinovich, Opt. Express 15 (2007) 7557.
[17] A.V. Tsarev, F. De Leonardis, V.M.N. Passaro, Opt. Express 16 (2008) 3101.
[18] O. Schwelb, Opt. Commun. 281 (2008) 1065.
[19] H.M. Stoll, IEEE Trans. Circ. Syst. CAS-26 (1979) 1065.
[20] S. Xiao, M.H. Khan, H. Shen, M. Qi, J. Lightwave Technol. 26 (2008) 228.
[21] O. Schwelb, I. Frigyes, J. Lightwave Technol. 19 (2001) 380.
[22] O. Schwelb, J. Lightwave Technol. 22 (2004) 1380.